Cryogenic Microjet Source for Orthotropic Beams of Ultralarge Superfluid Helium Droplets

Robert E. Grisenti and J. Peter Toennies

Max-Planck-Institut für Strömungsforschung, Bunsenstraße 10, 37073 Göttingen, Germany

(Received 12 December 2002; published 9 June 2003)

Liquid ^{4}He at pressures $P_0 = 0.5$–30 bars and temperatures $T_0 = 1.5$–4.2 K is discharged into vacuum through two different 2 μm nozzles. The velocities of the beam of particles obey the Bernoulli equation down to 15 m/sec. With decreasing T_0 and increasing P_0 the velocity and angular distributions become exceedingly narrow with $\Delta v/v \lesssim 1\%$ and $\Delta\vartheta \lesssim 1$ mrad. Optical observations indicate that the beam consists of micron-sized droplets ($N \gtrsim 10^9$ atoms). This new droplet source provides opportunities for novel experimental studies of superfluid behavior.

DOI: 10.1103/PhysRevLett.90.234501 PACS numbers: 47.27.Wg, 39.10.+j, 47.55.Bx, 67.40.Hf

Large superfluid ^{4}He droplets with 10^3–10^8 atoms have found important applications in molecular spectroscopy [1], for trapping single electrons which form bubbles [2] and for studying the frictionless motion of atoms in a superfluid [3]. In the past very large droplets with more than 10^4 atoms have been formed in supercritical expansions into vacuum of liquid He I with source pressures P_0 and temperatures T_0 in the ranges of 8–20 bars and 5–10 K, respectively [4] and are predicted to have evaporatively cooled temperatures of about 0.37 K [1]. The above experiments suffer from two drawbacks: (1) the broad droplet size distributions and (2) their rigidly fixed temperatures [1]. The exponential size distributions have been explained [4,5] in terms of fragmentation resulting from rapid expansion strains using theories for the cosmological "big bang" [6], as well as for fragmentation of nuclear matter or blast shattering of oil shale and cavitation induced fuel spraying. Experiments with water jets [7] or cryogenically cooled liquids [8] indicate, on the other hand, Rayleigh oscillation-induced breakup of a liquid jet into a sequence of large monodisperse droplets. The present experiments were designed to find Rayleigh breakup of liquid helium jets to obtain an orthotropic beam of ultralarge monodisperse droplets.

Although the different modes of liquid jet breakup have been extensively studied, at present no straightforward general theory, especially for microjets, is currently available [9]. Liquid helium offers many unique advantages including a wide range of temperatures down to 0 K and pressures up to solidification at about 25 bars. The superfluid, below $T_\lambda \approx 2.2$ K, is ideally inviscid and irrotational and its frictionless mass flow has been extensively studied at low pressure differentials ($\lesssim 100$ mbar) and low flow velocities ($v \lesssim 1$ m/sec) within long narrow channels or through small orifices [10]. For large Reynolds numbers $\mathrm{Re} > 1200$ ($\mathrm{Re} = \rho_0 d_0 v/\mu$, where ρ_0 is the density, d_0 is the nozzle diameter, and μ is the viscosity coefficient) there are only a few experiments largely motivated by the use of liquid helium as a fluid in high Reynolds number "wind tunnels" [11] or in connection with understanding the relationship between classical and quantum turbulence [12]. At $\mathrm{Re} \sim 10^5 - 2 \times 10^7$ one study [13] indicates classical fluid behavior.

In the present experiments the liquid was discharged into vacuum at $P_0 = 0.5$–30 bars using lower source temperatures of $T_0 = 1.5$–4.2 K than previously, thereby spanning the superfluid transition. The resulting beam of particles was characterized with time-of-flight (TOF) and angular distributions. The apparatus differs in two respects from that used previously [14]. (1) The temperature of the source, which was attached to a liquid helium bath cryostat, was measured and stabilized to within about ± 0.01 K by regulating the vapor pressure above the liquid helium bath. Because of radiation losses at the nozzle the actual temperature is higher by about 0.1 K than the measured one. The inlet gas pressure P_0 was regulated to ± 0.2 bars from the outside and the ultrapure ^{4}He was then liquefied by passing the feed line through the cryostat bath. (2) The ϑ angle seen by the detector with respect to the nozzle axis was scanned by rotating the entire cryostat via a stepping motor with angular increments of $\simeq 0.01$ mrad around its vertical axis which passes through the orifice opening. The ϕ angle was adjusted by mechanically tilting the flight tube around an axis at 90° to that of the cryostat. These adjustments were needed to aim the highly collimated beam into the detector and compensate for gravitational deflection of the slow beams.

The particles were detected by a differentially pumped mass spectrometer detector located 120 cm from the orifice. Most measurements were made at mass 8 amu and are sensitive only to clusters and not to atoms. The time-of-flight resolution is limited by the chopper slit width (1.5 mm) and effective ionizer length (≈ 5 mm) and can be reliably estimated to be about 0.8%. A 25 μm wide slit provided an angular resolution of 0.02 mrad. One nozzle was a 2 μm diameter, 3 μm long orifice and the other a large aspect-ratio silica pipette which is tapered from a 20 μm inner diameter over a distance of 0.23 mm to a 2 μm opening.

In Figs. 1(a)–1(c) the data at $P_0 = 3$ bars are summarized as a function of the source temperature. The velocities measured with the orifice did not change on passing through T_λ, but with the pipette they are consistently lower and, moreover, drop further by about 10% below T_λ [Fig. 1(a)]. The velocity and angular half-widths are narrowest for source temperatures of $T_0 \leq 1.9$ K for the pipette and $T_0 \leq 2.6$ K for the orifice. Since the measured velocity half-widths equal the estimated apparatus TOF resolution, the true half-widths are expected to be considerably narrower. The angular distribution narrows to a half-width of about 1 ± 0.5 mrad and is related approximately to the velocity half-width by $\Delta\vartheta \approx \Delta v/v$, indicating that the small spread in the velocities is the same parallel and normal to the beam direction. Surprisingly, at $T_0 \simeq 2.0$ K which, within the experimental accuracy, is equal to $T_\lambda(3 \text{ bars}) \simeq 2.12$ K, both the velocity and angular half-widths for orifice jets exhibit distinct maxima not seen with the pipette.

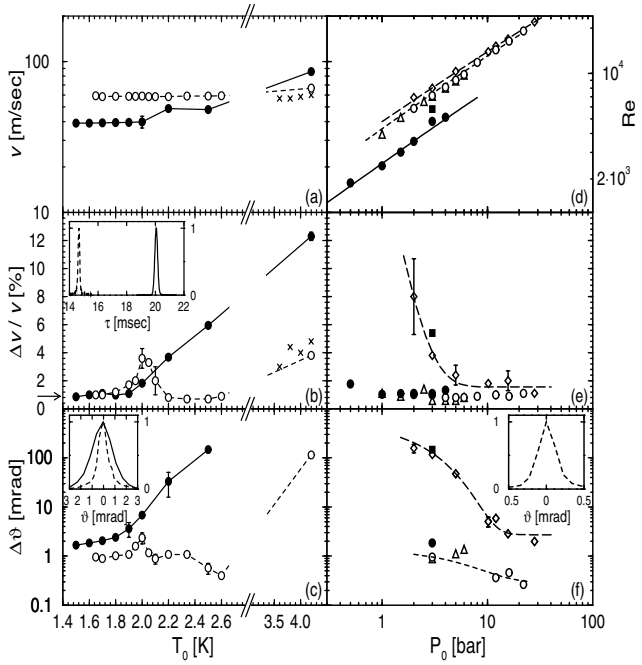

FIG. 1. The mean beam speeds v, relative widths $\Delta v/v$, and angular FWHM $\Delta\vartheta$'s measured with the mass spectrometer set on mass 8 amu as a function of the source temperature T_0 at $P_0 = 3$ bars (a)–(c) with the pipette (black circle) and with the orifice (white circle), and as a function of source pressure P_0 (d)–(f) at $T_0 = 1.60$ K (black circle) and 2.5 K (black square) with the pipette and at $T_0 = 1.65$ K (white circle), 2.34 K (triangle), and 4.2 K (diamond) with the orifice. The crosses ($\times$) in (a) and (b) are previous results from Ref. [14] measured with a 5 μm orifice at $P_0 = 2.3 \pm 0.2$ bar. Typical TOF and angular distributions, measured at $T_0 = 1.7$ K, are shown in the insets in (b) and (c) as a dashed line for the orifice and a solid line for the pipette. The arrow in (b) indicates the TOF resolution of the apparatus. The lines in (d) are least-square fits to the Bernoulli equation (see text). Those in (e) and (f) are guides to the eye. The inset in (f) shows the narrowest angular profile measured with the orifice at $P_0 = 22$ bars and $T_0 = 1.65$ K.

Figures 1(d)–1(f) show the source pressure dependencies of the mean velocities and the velocity and angular half-widths at source temperatures $T_0 = 1.65$, 2.43, and 4.2 K with the orifice and at $T_0 = 1.6$ K and $T_0 = 2.5$ K with the pipette. The straight lines in Fig. 1(d) are calculated with the Bernoulli formula $v = C\sqrt{2P_0/\rho_0}$ using the densities ρ_0 corresponding to the source pressures and temperatures. The best fit discharge coefficients are $C \simeq 1.0$ for the orifice independent of T_0. For the pipette $C \simeq 0.77$ for $T_0 > T_\lambda$ and $C \simeq 0.59$ for $T_0 < T_\lambda$. The smaller discharge coefficient found for the pipette is consistent with the buildup of a turbulent boundary layer. For turbulent flow with $\text{Re} \geq 2300$ [see right scale in Fig. 1(d)] the flow distance needed for formation of a stationary boundary layer in a channel is given by $L/d_0 \approx 4.4\text{Re}^{1/6} \geq 16$ [15]. Thus in the pipette turbulence will be fully developed, whereas in orifice flow with $L/d_0 \approx 1$ turbulence will be less important.

The measured lowest velocity of 15 m/sec ($P_0 = 0.5$ bar) was limited by partial loss of the beam by the large gravity deflection of 20 mm. Whereas the velocity half-widths [Fig. 1(e)] at $T_0 = 1.60$ K with the pipette and at 1.65 and 2.34 K with the orifice show no significant dependence on pressure up to solidification, the results at $T_0 = 4.2$ K show a pronounced exponential decrease in width with increasing pressures, leveling off to $\Delta v/v \simeq 1\%$, which again is about equal to the apparatus resolution. The angular widths at $T_0 = 4.2$ K show a corresponding decrease with P_0.

The extreme narrowing of both distributions is considered as evidence for the transition from cavitation induced fragmentation to Rayleigh breakup into large droplets. This could be confirmed by direct microscope observations of a several cm long sharply defined "white" filament (Fig. 2) made with the beam illuminated slightly off from the line of sight by a commercial halogen lamp (average wavelength $\simeq 950$ nm). Since backward scattering was completely suppressed Rayleigh-Gans theory [16] suggests that the beam consists of large droplets with $kR \gtrsim 1.5$, thereby providing a lower limit on the droplet radius R of about 0.25 μm ($N \approx 1.4 \times 10^9$). This rough estimate is consistent with the droplet sizes of $R \approx d_0$ predicted for Rayleigh breakup [17]. According to this theory inertial and surface tension forces lead to an exponential growth of small axisymmetric disturbances until they reach a size comparable to the jet radius. The breakup length ℓ is then given by $\ell \simeq 12v[(\rho_0 d_0^3/\sigma)^{1/2} + 3\mu d_0/\sigma]$ [18]. The predicted flight time prior to Rayleigh breakup of the contiguous helium jet ($d_0 = 2$ μm, $P_0 = 3$ bars) is $\tau_0 = \ell/v \simeq 5 \times 10^{-5}$ sec and the length of the liquid filament is $\simeq 3$ mm.

Thus under these new conditions other disintegration processes are largely suppressed despite the rapid dropoff

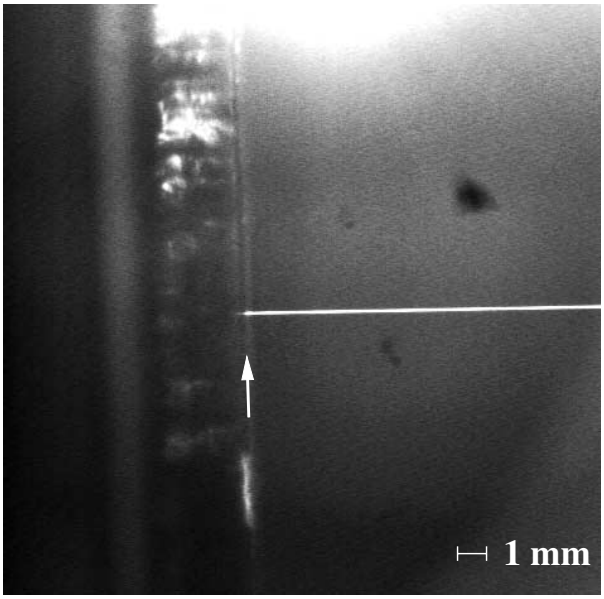

FIG. 2. Microscope photograph of the droplet beam with $P_0 = 3$ bars and $T_0 = 1.7$ K. The beam is illuminated by a halogen lamp off from the line of sight. The nozzle used for the optical observations, located about 2.5 mm behind the 2 cm diameter opening of the outer copper radiation shield (indicated by the white arrow), had a larger diameter of 5 μm.

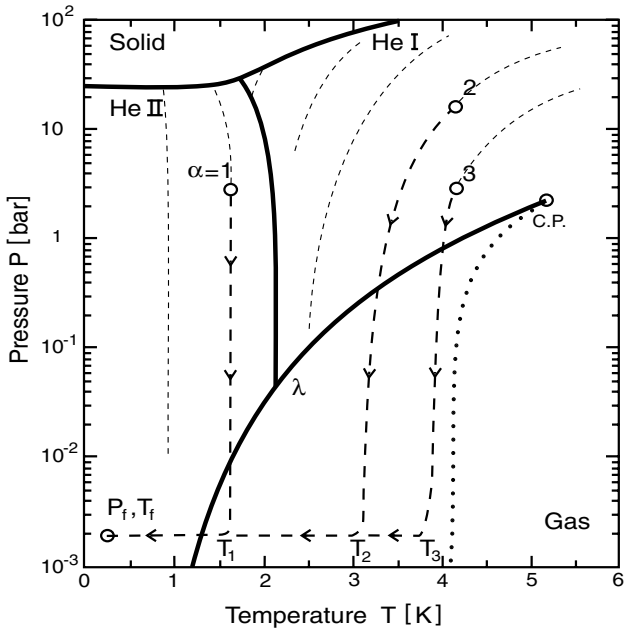

FIG. 3. Schematic diagram showing the two-step model for the state changes accompanying the expansions for $T_0 = 1.65$ K, $P_0 = 3$ bars ($\alpha = 1$), and for $T_0 = 4.2$ K at $P_0 = 15$ bars ($\alpha = 2$) and $P_0 = 3$ bars ($\alpha = 3$). The downward trajectories (thick dashed lines) follow the isentropes (thin dashed lines). The dotted line shows the homogeneous nucleation line based on the standard theory for the present experiments $V\tau \simeq 1.2 \times 10^{-13}$ cm^3 sec [20]. Since fragmentation is observed for the $\alpha = 3$ but not for the $\alpha = 2$ trajectory the nucleation line for the helium microjet lies between them and is shifted to lower temperatures.

in the pressure from P_0 to an internal surface tension induced pressure of $P_f = 2\sigma/d_0 \simeq 2$ mbar. For orifice flow the pressure drop occurs within a time given by $\tau_P \approx d_0/c \simeq 10^{-8}$ sec, where $c = 240$ m/sec is the speed of sound. For the pipette τ_P is considerably greater because of the pressure gradient inside the channel. In comparison the calculated evaporative cooling times for the liquid jet [19] are more than an order of magnitude larger. Thus for the orifice the expansion is expected to proceed in two distinct steps. As shown for three examples in Fig. 3 first the pressure and temperature fall along an isentrope from $(P_0^{(\alpha)}, T_0^{(\alpha)})$ to a metastable liquid state at (P_f, T_α) ($\alpha = 1, 2, 3$). By evaporative cooling the temperature then drops rapidly from T_α to T_f, which invariably is calculated to be about 0.5 K after 5×10^{-5} sec, at which time Rayleigh breakup occurs. The corresponding times for droplets are only about 30% shorter.

The pressure dependence of the velocity and angular half-widths at $T_0 = 4.2$ K provides a rather precise determination of the effective threshold temperature T_n for homogeneous nucleation in the orifice microjet. At $P_0 = 3$ bars, where the beam is extensively fragmentation broadened, the expansion isentrope for $T_0 = 4.2$ K ($\alpha = 3$) corresponds to $T_3 \approx 3.8$ K (see Fig. 3), whereas the narrow jet at $P_0 = 15$ bars ($\alpha = 2$) corresponds to $T_2 \approx 3.2$ K, and T_n appears to lie between these limits. According to the standard nucleation theory T_n depends on $V\tau$, the product of the volume V and time τ characteristic of the experiment [21]. For the present microjet, by assuming $\tau = \tau_0$ and $V = \pi d_0^2 \ell/4 \simeq 2.4 \times 10^{-9}$ cm^3, the expected threshold temperature is about 4.2 K [20] (Fig. 3), about 0.1 K higher than in previous bulklike experiments [22]. Since the dependence of T_n on $V\tau$ is very weak, the observed reduction in threshold cannot be explained in terms of an uncertainty in our V and τ and must be thus related to some other mechanism. Fragmentation via cavitation due to enclosed gases can be ruled out since liquid He is exceedingly pure: all foreign substances, except ^{3}He, are frozen out. Possibly the large surface to volume ratio and the turbulent boundary layer may play a role.

A very interesting observation is the distinct maxima found in both the velocity and angular distributions at $P_0 = 3$ bars, $T_0 \simeq 2.0$ K [Figs. 1(b) and 1(c)] which coincides within the experimental accuracy with $T_\lambda(3 \text{ bars}) \simeq 2.12$ K. Since the velocity spread Δv, expressed in terms of an effective temperature, is proportional to $\sqrt{kT_{\text{eff}}}$ the observed factor of 4 increase in Δv corresponds to a factor of 16 increase in T_{eff}. The calculated cooling rate, the time dependence of the temperatures of both the jet and the droplets, and the total number of evaporated atoms reveal, however, a regular behavior at T_λ, and therefore the maxima cannot be explained in terms of a temperature increase.

One possible explanation, which has been proposed in connection with a similar anomaly in cavitation experiments at negative pressures [23], assumes that quantized vortices are created and act as nucleation centers [24]. Moreover, at T_λ the vortex core is also expected to diverge[25]. More recently Williams has shown that at T_λ the diameter of vortex loops diverges and the density of vortices rises sharply [26]. A related mechanism which is fully consistent with the present results, although highly speculative, is the enhanced creation of vortices by the Kibble-Zurek mechanism [27].

In summary, the present experiments provide evidence for the cavitation nucleation threshold in normal and superfluid high Reynolds numbers liquid helium microjets. Beyond the threshold P_0, T_0 conditions the liquid jet after a short distance breaks up into an orthotropic beam of ultralarge droplets with diameters greater than 0.25 μm containing at least 10^9 atoms. The anticipated uniform droplet sizes will eliminate heterogeneous broadening of the spectral features of embedded molecules in superfluid ^{4}He droplets[1]. Much larger objects can be investigated and surface effects, which scale as R^{-1}, will be considerably reduced [28]. Moreover, as already demonstrated with beams of H_2 droplets [29] the temperatures of such large droplets can be raised and regulated by equilibration to a predetermined local ambient pressure of the same gas. Rapid equilibration is expected because of the short evaporation times of $\sim 10^{-7}$ sec. In addition, low velocities down to 15 m/sec or even less, which are well below the Landau critical velocity of 58 m/sec, can now be achieved and open up new opportunities for studying superfluid passage of particles through the droplets [3] or searches for direct evidence for off-diagonal long-range order of the condensate [30]. Because of the high directionality the brilliance of $\sim 10^{22}$ atoms/sec sr is greater by 2–3 orders of magnitude than for conventional gas nozzle sources. The greatly increased brilliance makes these beams ideal targets for x-ray production via laser induced implosion [8] or for atomic and nuclear physics experiments at high energies [29].

We thank O. Kornilov, L. Kraus, J. Pick, and H. Wuttke for assistance and G. Valaskovich for providing the pipettes. We also thank S. Balibar, M. Barranco, W. F. Vinen, and G. A. Williams for extensive discussions and correspondence on cavitation and vortex creation. We are also grateful to K. Burnett, H. Chaves, B. Doak, M. Faubel, and A. F. Vilesov for discussions.

[1] J. P. Toennies, A. F. Vilesov, and K. B. Whaley, Phys. Today **54**, No. 2, 31 (2001).
[2] M. Fárnik, U. Henne, B. Samelin, and J. P. Toennies, Phys. Rev. Lett. **81**, 3892 (1998).
[3] J. Harms and J. P. Toennies, Phys. Rev. Lett. **83**, 344 (1999).
[4] E. L. Knuth and U. Henne, J. Chem. Phys. **110**, 2664 (1999).
[5] W. T. Ashurst and B. L. Holian, Phys. Rev. E **59**, 6742 (1999).
[6] B. L. Holian and D. E. Grady, Phys. Rev. Lett. **60**, 1355 (1988).
[7] M. Faubel, S. Schlemmer, and J. P. Toennies, Z. Phys. D **10**, 269 (1988).
[8] O. Hemberg, B. A. M. Hansson, M. Berglund, and H. M. Hertz, J. Appl. Phys. **88**, 5421 (2000).
[9] U. Moseler and U. Landman, Science **289**, 1165 (2000).
[10] For an excellent review, see W. E. Keller, *Helium-3 and Helium-4* (Plenum, New York, 1969), Chap. 8.
[11] *High Reynolds Number Flows Using Liquid and Gaseous Helium*, edited by R. J. Donnelly (Springer, New York, 1991).
[12] W. F. Vinen and J. J. Niemala, J. Low Temp. Phys. **128**, 167 (2002).
[13] S. Fuzier, B. Baudouy, and S.W. van Sciver, Cryogenics **41**, 453 (2001).
[14] J. Harms, J. P. Toennies, and E. L. Knuth, J. Chem. Phys. **106**, 3348 (1997).
[15] I. H. Shames, *Mechanics of Fluids* (McGraw-Hill, New York, 1982), p. 359 ff.
[16] H. C. van de Hulst, *Light Scattering by Small Particles* (Dover, New York, 1981).
[17] J. Eggers, Rev. Mod. Phys. **69**, 865 (1997).
[18] M. J. McCarthy and N. A. Molloy, Chem. Eng. J. (London) **7**, 1 (1974).
[19] Calculated assuming a bulk heat capacity. See, e.g., D. O. Edwards and W. F. Saam, in *Progress in Low Temperature Physics*, edited by D. F. Brewer (North-Holland, Amsterdam, 1978), Vol. VIIa, Chap. 4, p. 314 ff.
[20] S. Balibar (private communication).
[21] S. Balibar, J. Low Temp. Phys. **129**, 363 (2002).
[22] D. N. Sinha, J. S. Semura, and L. C. Brodie, Phys. Rev. A **26**, 1048 (1982).
[23] M. S. Pettersen, S. Balibar, and H. J. Maris, Phys. Rev. B **49**, 12 062 (1994).
[24] H. J. Maris, J. Low Temp. Phys. **94**, 125 (1995).
[25] C. F. Barenghi, R. J. Donnelly, and W. F. Vinen, J. Low Temp. Phys.. **52**, 189 (1983).
[26] G. A. Williams, Phys. Rev. Lett. **82**, 1201 (1999).
[27] W. H. Zurek, Nature (London) **317**, 505 (1985). According to this theory an extremely high vortex density is expected to be created on rapid passage of liquid ^{4}He through the λ line. The expansion isentropes near the λ line have a positive slope dP/dT, whereas the λ line has a negative slope so that a crossing through the λ line is expected to take place for $T_0(P_0) \gtrsim T_\lambda(P_0)$. The lack of a similar effect in pipette flow is consistent with the larger channel passage time for which the density of vortices formed is expected to be much smaller.
[28] K. K. Lehmann, Mol. Phys. **97**, 645 (1999).
[29] B. Trostell, Nucl. Instrum. Methods Phys. Res., Sect. A **362**, 41 (1995)
[30] J.W. Halley, C. E. Campbell, C. F. Giese, and K. Goetz, Phys. Rev. Lett. **71**, 2429 (1993); A. Setty, J.W. Halley, and C. E. Campbell, Phys. Rev. Lett. **79**, 3930 (1997).